Anti-trypanosomal activities and structural chemical properties of selected compound classes

Alicia Ponte-Sucre, Heike Bruhn, Tanja Schirmeister, Alexander Cecil, Christian R. Albert, Christian Buechold, Maximilian Tischer, et al.

Parasitology Research
Founded as Zeitschrift für Parasitenkunde

ISSN 0932-0113
Volume 114
Number 2

Parasitol Res (2015) 114:501-512
DOI 10.1007/s00436-014-4210-4

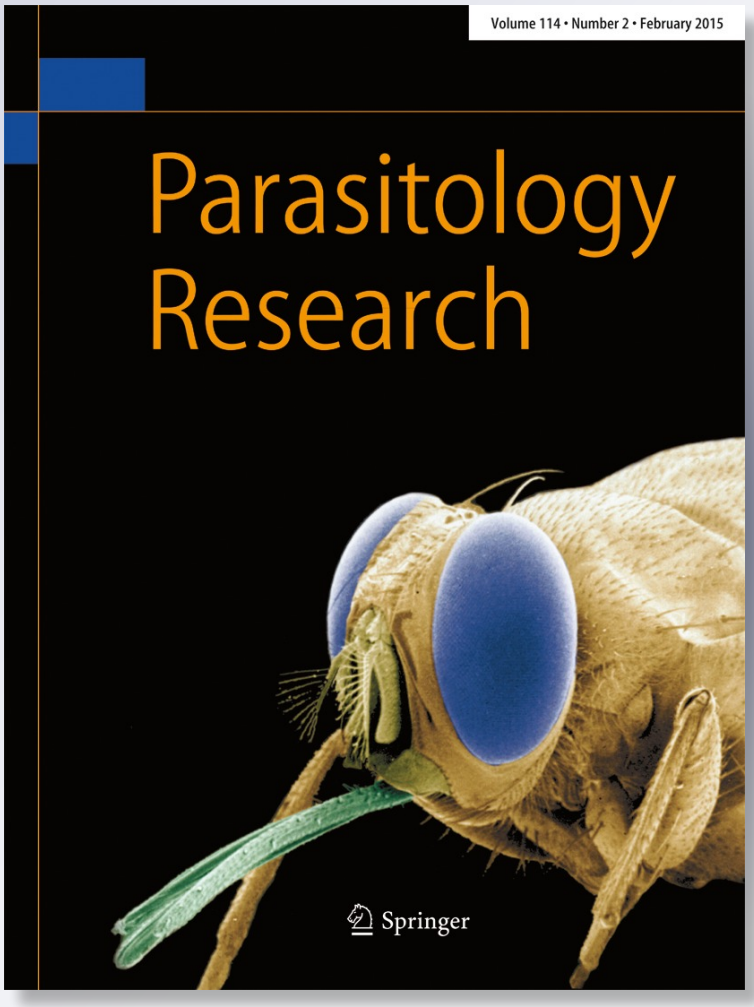

Springer

Parasitol Res (2015) 114:501–512
DOI 10.1007/s00436-014-4210-4

ORIGINAL PAPER

Anti-trypanosomal activities and structural chemical properties of selected compound classes

Alicia Ponte-Sucre · Heike Bruhn · Tanja Schirmeister · Alexander Cecil · Christian R. Albert · Christian Buechold · Maximilian Tischer · Susanne Schlesinger · Tim Goebel · Antje Fuß · Daniela Mathein · Benjamin Merget · Christoph A. Sotriffer · August Stich · Georg Krohne · Markus Engstler · Gerhard Bringmann · Ulrike Holzgrabe

Received: 16 October 2014 / Accepted: 30 October 2014 / Published online: 23 November 2014

Abstract Potent compounds do not necessarily make the best drugs in the market. Consequently, with the aim to describe tools that may be fundamental for refining the screening of candidates for animal and preclinical studies and further development, molecules of different structural classes synthesized within the frame of a broad screening platform were evaluated for their trypanocidal activities, cytotoxicities against murine macrophages J774.1 and selectivity indices, as well as for their ligand efficiencies and structural chemical properties. To advance into their modes of action, we also describe the morphological and ultrastructural changes exerted by selected members of each compound class on the parasite *Trypanosoma brucei*. Our data suggest that the potential organelles targeted are either the flagellar pocket (compound **77**, *N*-Arylpyridinium salt; **15**, amino acid derivative with piperazine moieties), the endoplasmic reticulum membrane systems (**37**, bisquaternary bisnaphthalimide; **77**, *N*-Arylpyridinium salt; **68**, piperidine derivative), or mitochondria and kinetoplasts (**88**, *N*-Arylpyridinium salt; **68**, piperidine derivative). Amino acid derivatives with fumaric acid and piperazine moieties (**4**, **15**) weakly inhibiting cysteine proteases seem to preferentially target acidic compartments. Our results suggest that ligand efficiency indices may be helpful to learn about the relationship between potency and

Electronic supplementary material The online version of this article (doi:10.1007/s00436-014-4210-4) contains supplementary material, which is available to authorized users.

A. Ponte-Sucre (✉)
Laboratory of Molecular Physiology, Institute of Experimental Medicine, School of Medicine Luis Razetti, Faculty of Medicine, Universidad Central de Venezuela, Caracas, Venezuela
e-mail: aiponte@gmail.com

H. Bruhn
Institute of Molecular Infection Biology, University of Würzburg, Josef-Schneider-Straße 2, 97080 Würzburg, Germany

T. Schirmeister · C. Buechold · M. Tischer · T. Goebel · B. Merget · C. A. Sotriffer · U. Holzgrabe (✉)
Institute of Pharmacy and Food Chemistry, University of Würzburg, Am Hubland, 97074 Würzburg, Germany
e-mail: u.holzgrabe@pharmazie.uni-wuerzburg.de

T. Schirmeister
Institute of Pharmacy and Biochemistry, University of Mainz, Staudinger-Weg 5, 55128 Mainz, Germany

A. Cecil
Department of Bioinformatics, University of Würzburg, Am Hubland, 97074 Würzburg, Germany

C. R. Albert · G. Bringmann
Institute of Organic Chemistry, University of Würzburg, Am Hubland, 97074 Würzburg, Germany

S. Schlesinger · A. Fuß · D. Mathein · A. Stich
Department of Tropical Medicine, Institute of Medical Mission, Salvator Straße 7, 97074 Würzburg, Germany

G. Krohne
Division of Electron Microscopy, Biocenter of the University of Würzburg, Am Hubland, 97074 Würzburg, Germany

M. Engstler
Department of Cell and Developmental Biology, University of Würzburg, Am Hubland, 97074 Würzburg, Germany

chemical characteristics of the compounds. Interestingly, the correlations found between the physico-chemical parameters of the selected compounds and those of commercial molecules that target specific organelles indicate that our rationale might be helpful to drive compound design toward high activities and acceptable pharmacokinetic properties for all compound families.

Keywords Compound design · Drug potency · Drug targets · Electron microscopy · Ligand efficiency · *Trypanosoma brucei*

Introduction

Human African trypanosomiasis (HAT) is caused by the unicellular protozoan parasites *Trypanosoma brucei gambiense* and *rhodesiense*. African trypanosomes are extracellular flagellated protozoa that prosper in blood and tissues of the mammalian hosts and are transmitted by the bite of tsetse flies. In its late stages, HAT induces terminal somnolence, a step in the disease that invariably leads to death if untreated (Brun et al. 2010).

Actual chemotherapies were developed decades ago and are characterized by their poor efficacy and serious side effects, meaning that alternative strategies to treat HAT are urgently required and new and effective drugs are needed (Steverding and Tyler 2005; Stich et al. 2013). However, the cost for identifying and developing new therapeutics is enormous; additionally, a high attrition rate produces the loss of candidates during the development process (Verkman 2004).

Trypanosoma (*T.*) *brucei* is a well-studied cell from many points of view, including its molecular genetics, metabolism, and cell structure (Field et al. 2004). It offers an exceptional opportunity in the identification of structures fundamental for a successful host cell infection and to guarantee pathogenesis. These targets may be used to guide the design of novel and optimized therapies and conduct drug discovery against these protozoan organisms. We analyzed various highly active families of compounds (for representative structural formulae, see Fig. 1; for SMILES strings, see Supplementary Material, Table 1), bisquaternary bisnaphthalimides designed as choline analogs, amino acids with fumaric acid and piperazine moieties, piperidine derivatives and simplified *N*-Arylpyridinium salts derived from *N*,*C*-coupled naphthylisoquinolines.

Naphthalimides exhibit high anti-tumoral activity probably due to their capacity to intercalate and interact with DNA (Braña and Ramos 2001; Sami et al. 2000). However, bisquaternary derivatives of these compounds (Bender et al. 2000; Muth et al. 2007) are not cytotoxic against mammalian cell lines. Furthermore, bisquaternary bisnaphthalimides exhibit anti-malarial activity in the low nanomolar range most likely due to their interference with membrane biosynthesis (Tischer et al. 2010). Their high activities against *T. brucei* demonstrate their potential as lead compounds to design drugs against parasites (Muth et al. 2007) that rely on de novo lipid biosynthesis (Smith and Bûtikofer 2010).

Naphthylisoquinoline alkaloids, naturally occurring plant-derived compounds isolated from tropical lianas from the families *Ancistrocladaceae* and *Dioncophyllaceae*, exhibit significant anti-trypanosomal and anti-leishmanial activities (Bringmann et al. 2003; Ponte-Sucre et al. 2007). *N*-Arylpyridinium salts as simplified analogs of *N*,*C*-coupled naphthylisoquinolines are selective against trypanosoma species without activity against *Leishmania* and not cytotoxic against J774.1 macrophages or L6 mouse cells (Ponte-Sucre et al. 2007; Ponte-Sucre et al. 2009).

The amino acid derivatives, containing fumaric acid and piperazine moieties, are active against trypanosoma. Piperidines and derivatives target enzymes of the polyamine pathway and may provide novel anti-trypanosomal options. Some of the evaluated candidates are active against *Trypanosoma brucei brucei* and *Plasmodium falciparum* and express low cytotoxicity against macrophages (Goebel et al. 2008). Their mode of action remains to be elucidated; however, it is well known that some of the amino acid compounds weakly inhibit cysteine proteases (Breuning et al. 2010).

Properties related to compound *a*bsorption, *d*-istribution, *m*etabolism, and *e*xcretion (ADME) are fundamental for refining the screening of potential candidates that should go into animal and preclinical studies and further development. In silico prediction of ADME properties provides an initial and inexpensive way to analyze compounds concomitant with their synthesis and biological testing (Hou et al. 2007). Among them, the "Lipinski rule of 5" (Lipinski et al. 2001) has become popular to tentatively identify compounds of reduced oral bioavailability caused by poor membrane permeability, i.e., absorption and low solubility in aqueous solutions.

ADME properties influence drug pharmacokinetics, pharmacodynamics, and mechanism(s) of action. Finally, it has been proposed that physico-chemical parameters of compounds delineate the relationship between chemical structure and biological functions (Efremov et al. 2007; Ponte-Sucre et al. 2012). Therefore, terms like ligand efficiency or ligand efficiency indices (LEi) have been defined to relate potency of compounds to their size and polarity (or hydrophobicity); they may guide drug discovery (Leeson and Springthorpe 2007).

To describe tools that may be useful to channel the search of compounds, and to understand their biological activity, as well as their fate within the organism, we

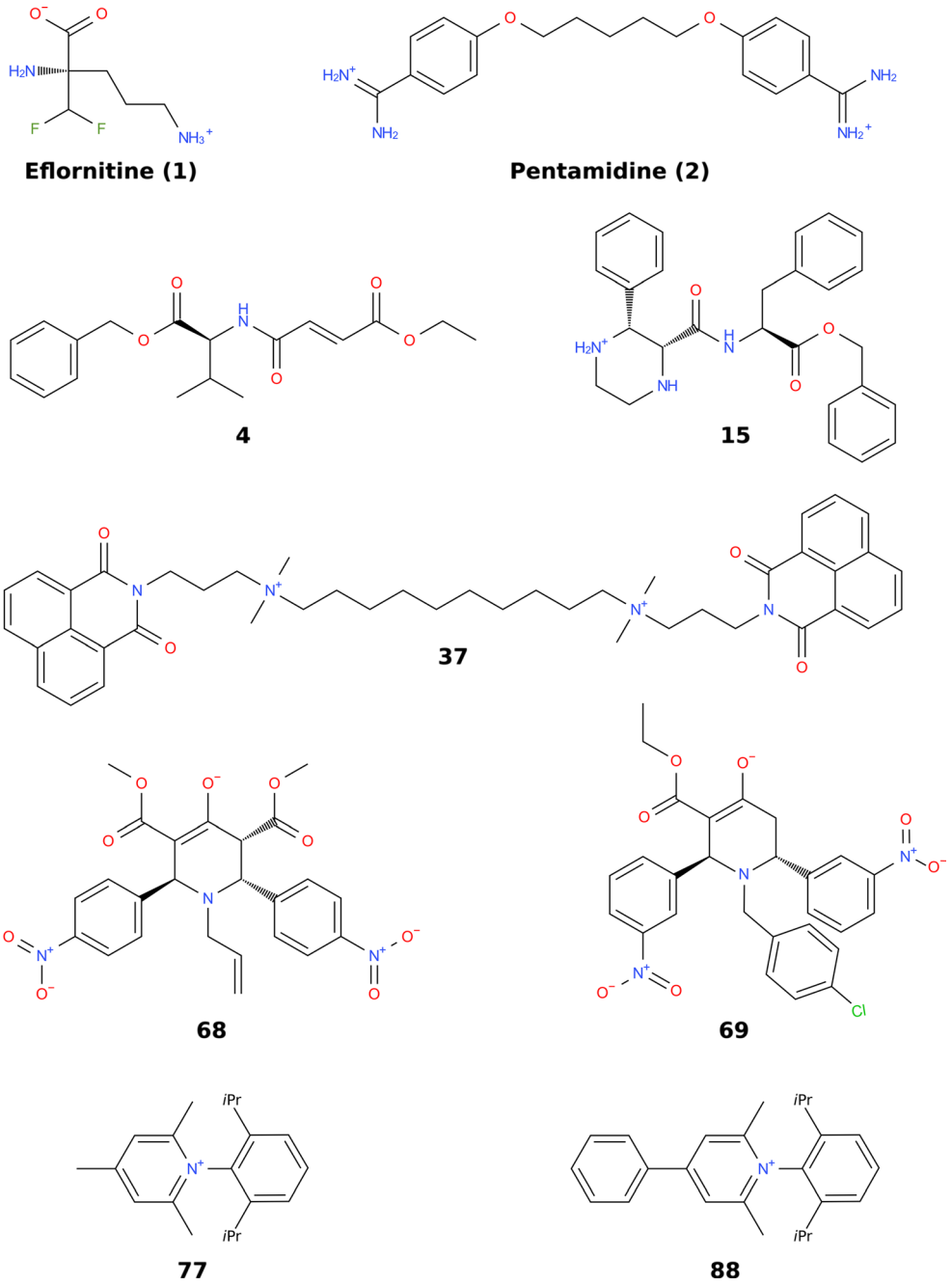

Fig. 1 Structures of the compounds used for the analysis. Amino acid derivative of fumaric acid 4; piperazine 15; bisquaternary bisnaphthalimide 37; piperidine derivatives 68 and 69; and *N*-Arylpyridinium salts 77 and 88

have 1. evaluated the morphological and ultrastructural effects exerted by selected anti-trypanosomal molecules on *T. brucei*; 2. identified the potential organelles targeted; 3. described their physico-chemical parameters; 4. compared our results with those exerted by pentamidine (**1**) and eflornitine (**2**), drugs with well-known mode of actions on *T. brucei*; and 5. analyzed the potential correlation that may exist between physico-chemical parameters of the compounds and their activity on parasite cells. Our results suggest that our rationale has been useful to drive compound design toward high activity and acceptable pharmacokinetic properties and indicate that LEi could be helpful for refining the screening of candidates that should go into further development.

Materials and methods

Materials for the synthesis of compounds

Starting materials for the synthesis of compounds were purchased from Sigma-Aldrich (Taufkirchen, Germany) and used without further purification. Sephadex LH-20 was obtained from Amersham Bioscience (Uppsala, Sweden). Organic

solvents were distilled and dried prior to use, using standard procedures.

General experimental procedures for the synthesis of compounds

Melting points were determined on a Reichert-Jung Thermovar hot plate (Reichert Optische Werke, Vienna, Austria) and are uncorrected. The nuclear magnetic resonance (NMR) spectra (^{1}H, 400 MHz and ^{13}C, 100 MHz) were recorded on a Bruker AMX 400 and Bruker a AV 400 (Bruker BioSpin, Rheinstetten, Germany), using deutero-chloroform (δ 7.24 and 77.23; Roth, Karlsruhe, Germany) as the solvent and the internal ^{1}H and ^{13}C standard. Electron ionization mass spectra were determined on a Finnigan MAT 8200 mass spectrometer (Thermo Electron Corporation, Whatman) in the positive mode (70 eV). ESI spectra were determined on a Bruker Daltonics micrOTOF-focus. FT-IR spectra were recorded on a Bio-Rad Pharmalyz IR and a Jasco FT-IR-410, both equipped with an ATR unit.

The bisquaternary bisnaphthalimide **37** was synthesized according to (Tischer et al. (2010)) and the piperidine derivative **68** according to (Goebel et al. (2008)).

Families of compounds

Figure 1 summarizes the structural formulae of the compounds selected for the morphological and ultrastrucural analysis:

i. Amino acid derivatives of fumaric acid, **4**, or of piperazine, **15**
ii. Bisquaternary bisnaphthalimides **37**
iii. Piperidine derivatives **68** and **69**
iv. *N*-Arylpyridinium salts **77** and **88**

The Simplified Molecular Input Line Entry System (SMILES) strings of all used compounds to determine Lei(s) are depicted in Table 1, Supplementary Material.

*Benzyl (S)-2-(E)-3-ethoxycarbonyl-acryloylamino) valinate ester (**4**)*

To a solution of 1.00 g (4.10 mmol) valine benzyl ester hydrochloride in 20 mL ethyl acetate, 828 mg (8.18 mmol) triethylamine were added at 0 °C. Separately, 1.30 g (9.03 mmol) monoethyl fumarate were activated with 903 mg (4.38 mmol) *N*,*N*'-dicyclohexyl carbodiimide (DCC) in 20 mL ethyl acetate. The precipitated *N*,*N*'-dicyclohexyl urea was filtered off and washed with ethyl acetate, and the filtrate was added dropwise to the solution of valine benzyl ester hydrochloride and triethylamine in ethyl acetate. The reaction mixture was stirred for 5 h in an ice bath. The organic layer was washed with brine (3×20 mL) and dried with sodium sulfate. Evaporation of the solvent yielded 460 mg (1.38 mmol, 37 %) as a yellowish viscous liquid. ^{1}H-NMR (400 MHz, $CDCl_3$) δ=0.88 (3H, d, *J*=6.8 Hz, CH(CH_3)$_2$), 0.92 (3H, d, *J*=7.1 Hz, CH(CH_3)$_2$), 1.29–1.32 (3H, t, *J*=7.1 Hz, CH_2CH_3), 2.19–2.25 (1H, m, C*H*(CH$_3$)$_2$), 4.22–4.27 (2H, q, *J*=7.2 Hz, CH_2CH$_3$), 4.69-4.72 (1H, m, C*H*CH(CH$_3$)$_2$), 5.12–5.22 (2H, m, CO_2CH_2Ph), 6.28 (1H, d, *J*=8.6 Hz, N*H*) 6.79–6.83 (1H, d, *J*=15.5 Hz, C*H*=CHCONH), 6.93–6.97 (1H, d, *J*=15.4 Hz, CH=C*H*-CONH), 7.32–7.38 (5H, m, Ar-H); ^{13}C-NMR (100 MHz, $CDCl_3$) δ=14.06 (CH_2CH_3), 17.63 (CHCH(*C*H$_3$)$_2$), 18.86 (CHCH(*C*H$_3$)$_2$), 31.45 (CH*C*-H(CH$_3$)$_2$), 57.32 (*C*HCH(CH$_3$)$_2$), 61.17 (CH_2CH_3), 67.21 (CO_2CH_2Ph), 128.3 (Ar-C), 128.5 (Ar-C), 128.6 (Ar-C), 130.9 (*C*H=CHCONH), 135.1 (CH=*C*HCONH), 135.9 (Ar-C), 163.5 (C=O), 165.5 (C=O), 171.5 (C=O); FT-IR [cm^{-1}]=3311, 3035, 2964, 2935, 1724, 1668, 1531, 1450, 1379, 1259, 696; mass spectrometry (MS) (electron spray ionization [ESI]) *m/z*333.2 [M]$^{+}$, 334.3 [M+H]$^{+}$, 356.3 [M+Na]$^{+}$, 689.3[2 M+Na]$^{+}$; LC-MS: R_t=19.7 min, purity: 98 %; $[\alpha]_D^{25\,°C}$=5.4° [c=0.74, $CHCl_3$].

*(S)-Benzyl-3-phenyl-2-[(3-phenylpiperazine-2-carbonyl) -amino] propionate (**15**)*

Four hundred sixty-six milligrams of (0.86 mmol) benzyl-(*S*)-2-{[(2*R*,3*R*)+(2*S*,3*S*)-1-(2-*tert*-butoxycarbonylaminoethyl)-3-phenylaziridine-2-carbonyl]-amino}-3-phenylpropionate (Buechold et al. 2011) was stirred with 2 mL trifluoroacetic acid in 8 mL dichloromethane for 2 h at room temperature to remove the Boc-protecting group. After the addition of 242 μl (1.72 mmol) diisopropylamine, the reaction mixture was stirred for several days in 7 mL dimethylformamide. The purification through a chromatographic system (silica gel, cyclohexane-ethylacetate 1:1, R_f: 0.12) delivered the piperazine **15** (1:1 mixture of the two diastereomers) as a yellowish viscous liquid (271 mg, 0.61 mmol, 71 %). ^{1}H-NMR ($CDCl_3$, 400 MHz) δ=2.30, 2.45, 2.66, and 3.04 (8H, 4×m, CH_2CH_2), 2.92–3.25 (2×2H, m, Phe-β-CH_2), 3.16(2×1H, m, C*H*-Ph), 4.83 and 4.95 (2×1H, m, Phe-α-C*H*), 5.04 (2×1H, m, C*H*-CO), 5.12 and 5.20 (2×2H, m, OBn-CH_2), 7.11 and 7.67 (2×1H, d, *J*=8.6,N*H*), 6.88–7.37 (30H, m, Ar-C*H*), 7.36 (2×1H, m, N*H*CH$_2$CH$_2$N*H*); ^{13}C-NMR ($CDCl_3$, 100 MHz) δ=36.72–39.98 (Phe-β-*C*H$_2$), 47.02, 47.57 (*C*H$_2$*C*H$_2$), 52.83, 53.32 (Phe-α-*C*H), 67.96 (OBn-*C*H$_2$), 68.55 (*C*H-Ph), 73.62, 73.87 (*C*H-CO), 127.2–129.5 (Ar-*C*H), 171.9–172.6 (*C*=O); FT-IR [cm^{-1}]=3309, 2924, 1737, 1660, 1515, 1178, 747, 698;

mass spectrum (ESI) *m/z* 558.5 $[M+H*TFA]^+$ (theoretical 443.55); $[\alpha]_D^{20\circ C}=-7.1°$ [*c*=0.62, MeOH].

*Ethyl 1-chlorobenzyl-4-hydroxy-2,6-bis-(3-nitrophenyl) -1,2,5,6-tetrahydropyridine-3-carboxylate (**69**)*

Compound **69** was synthesized according to a modified method (cf. Goebel et al. 2008). Fifteen millimoles of trioxotetrahyropyran were dissolved in absolute ethanol and stirred for 1 h. The solution was cooled to −20 °C, and 30 mmol 3-nitrobenzaldehyde, dissolved in tetrahydrofuran, and 15 mmol *p*-chlorobenzylamine were simultaneously added and stirred for another 2 h. After storage for 3 days at 5 °C, the formed precipitate was filtered off and the filtrate was treated with ice water till a white precipitate was formed. The precipitate was filtered off and washed with cold Et_2O to afford 900 mg (11 %) of the piperidine **69** as colorless crystals. Melting point, 174 °C; ^{1}H-NMR (400 MHz, $CDCl_3$) δ=0.96 (3H, t, *J*=7.1, OCH_2CH_3), 2.75 (1H, dd, *J*=18.0, *J*=4.9, $H5_{eq}$), 2.93 (1H, dd, *J*=18.0, *J*=11.8, $H5_{ax}$), 3.36 (2H, s, CH_2-Ar), 3.92–4.34 (3H, m, OCH_2 and H6), 4.66 (1H, s, H2), 7.20–7.32 (4H, m, H3b/5b and H2b/6b), 7.32–7.63 (4H, m, Ar-H), 8.04–8.10 (2H, m, Ar-H), 8.21 (1H, s, Ar-H), 8.23 (1H, s, Ar-H), 12.61 (1H, s, OH); ^{13}C-NMR (100 MHz, $CDCl_3$) δ=14.2 (CH_3), 28.1 (C5), 49.7 (CH_2-Ar), 53.0 (OCH_2), 57.5 (C6), 61.0 (C2), 96.2 (C3), 122.1 (Ar-C), 122.6 (Ar-C), 123.0 (Ar-C), 123.2 (Ar-C), 128.9 (Ar-C), 129.5 (Ar-C), 129.8 (Ar-C), 130.4 (Ar-C), 133.2 (Ar-C), 133.6 (Ar-C), 133.7 (Ar-C), 137.8 (Ar-C), 142.3 (Ar-C), 145.0 (Ar-C), 148.4 (Ar-C), 148.6 (Ar-C), 169.1 (C4), 171.7 (C=O); FT-IR [cm^{-1}]=2964, 1738, 1660, 1645, 1608, 1520, 1461, 1422, 1341, 1269,1239, 1151, 1110, 1052, 858, 821, 763, 731; combustion analysis ($C_{27}H_{24}ClN_3O_7$): calculated CHN content (calcd) C 60.95, H 4.50, N 7.81; found C 60.35, H 4.42, N 7.95.

*N-(2',6'-diisopropylphenyl)-2,4,6-trimethylpyridinium tetrafluoroborate (**77**)*

The pyridinium salt **77** was produced by stirring a mixture of 100 mg (0.48 mmol) 2,4,6-trimethylpyrylium tetrafluoroborate (Balaban and Boulton 1969) and 84.4 mg (0.48 mmol) 2,6-diisopropylaniline in 3 mL MeOH for 4 h under reflux. After the addition of 5 mL Et_2O, the white solid was filtered and washed with Et_2O. Recrystallization from a mixture of methanol-Et_2O gave 162 mg (0.44 mmol, 92 %) as colorless crystals. Melting point, 244 °C; ^{1}H-NMR (400 MHz, $CDCl_3$) δ=1.16 (12H, d, *J*=6.8 Hz, CH_3), 1.98 (2H, sep, *J*=6.8 Hz, CH), 2.37 (6H, s, CH_3), 2.73 (3H, s, CH_3), 7.43 (2H, d, *J*= 7.8 Hz, Ar-H), 7.61–7.65 (1H, m, Ar-H), 7.89 (2H, s, Ar-H); ^{13}C-NMR (100 MHz, $CDCl_3$) δ=21.67 (CH_3), 22.35 (CH_3), 24.30 (CH_3), 28.55 (CH), 126.6 (Ar-C), 129.3 (Ar-C), 132.6 (Ar-C), 133.9 (Ar-C), 143.1 (Ar-C), 154.9 (Ar-C), 161.5 (Ar-C); FT-IR [cm^{-1}]=3449, 2966, 2931, 2871, 1637, 1563, 1476, 1461, 1389, 1318, 1279, 1209, 1096, 1053, 933, 857, 825, 777; mass spectrometry (MS) (electron impact [EI]) *m/z* (%)= 282 $[M]^+$ (22), 281 $[M-1]^+$ (84), 267 $[M-CH_3]^+$ (22), 266 (100), 239 $[M-C_3H_7]^+$ (14), 238 (66), 195 (16), 121 $[M-C_{12}H_{17}]^+$ (15), 49 (20), 44 (26); mass spectrum (ESI)*m/z* 282.22163 $[M]^+$ (theoretical 282.22163).

*N-(2',6'-diisopropylphenyl)-2,6-dimethyl-4-phenylpyridinium tetrafluoroborate (**88**)*

A mixture of 100 mg (0.37 mmol)4-phenyl-2,6-dimethylpyrylium tetrafluoroborate (Rippert and Hansen 1995) and 65.1 mg (0.37 mmol)2,6-diisopropylaniline was dissolved in 3 mL MeOH and refluxed for 4 h. After the addition of 5 mL Et_2O, the white solid was filtered and washed with Et_2O. The mother liquor was diluted with methanol and purified on a Sephadex-LH20 column with methanol as the eluent. The crude products were combined and recrystallized from methanol-Et_2O to afford 143 mg (0.33 mmol, 90 %) of the pyridinium salt **88** as colorless crystals. Melting point, 297 °C; ^{1}H-NMR (400 MHz, $CDCl_3$) δ=1.17 (12H, d, *J*=6.8 Hz, CH_3), 2.04 (2H, sep, *J*=6.8 Hz, CH), 2.47 (6H, s, CH_3), 7.45 (2H, d, *J*=7.8 Hz, Ar-H), 7.54–7.56 (3H, m, Ar-H), 7.63–7.67 (1H, m, Ar-H), 8.03–8.07 (2H, m, Ar-H), 8.29 (2H, s, Ar-H); ^{13}C-NMR (100 MHz, $CDCl_3$) δ=22.04 (CH_3), 24.33 (CH_3), 28.66 (CH), 125.0 (Ar-C), 126.6 (Ar-C), 128.8 (Ar-C), 130.1 (Ar-C), 132.6 (Ar-C), 132.8 (Ar-C), 133.5 (Ar-C), 134.0 (Ar-C), 143.0 (Ar-C), 156.0 (Ar-C), 157.6 (Ar-C); FT-IR [cm^{-1}]=2968, 2931, 2874, 1633, 1561, 1462, 1443, 1388, 1367, 1326, 1274, 1205, 1091, 1045, 1034, 896, 818, 772, 734; mass spectrum (EI) *m/z* (%)=344 $[M]^+$ (13), 343 $[M-1]^+$ (39), 329 $[M-CH_3]^+$ (27), 328 (100), 301 $[M-C_3H_7]^+$ (16), 300 (63), 183 $[M-C_{12}H_{17}]^+$ (6); mass spectrum (ESI) *m/z* 344.23745 $[M]^+$ (theoretical 344.23728).

Analysis of in vitro anti-trypanosomal activity

Bloodstream forms of the monomorphic *T. brucei* (TC-221) were cultured in Baltz medium in a humid atmosphere at 37 °C in 5 % CO_2. The medium was supplemented with 16.7 % heat-inactivated fetal bovine serum, 16 U mL^{-1} penicillin, 16 μg mL^{-1} streptomycin, and 0.0001 % β-mercaptoethanol. Compound bioactivity was determined using the Alamar Blue® assay, as previously described (Muth et al. 2007).

Analysis of in vitro cytotoxic activity

The macrophage cell line J774.1 was maintained in complete medium (Click RPMI 1640 medium supplemented with 10 % heat-inactivated FCS, 2 mM L-glutamine, 10 mM HEPES buffer (pH 7.2), 60 μg mL^{-1} penicillin, and 20 μg mL^{-1}

gentamycin). For the experimental procedures, cells were detached from the flasks with a rubber policeman, washed twice with PBS, and suspended at 2×10^6 cells mL^{-1} in complete medium. Compound bioactivity was determined using the Alamar Blue® assay, as previously described (Ponte-Sucre et al. 2007).

Analysis of morphological changes in parasites exposed to the drugs

T. brucei cultures at their exponential growth phase (10^5 cells mL^{-1}) were incubated with compounds or pentamidin (as reference compound) at their IC_{50} for different periods. Every 90 min an aliquot of the cells was collected and stained with Giemsa®, using standard protocols.

Analysis of ultrastructural changes in parasites exposed to the drugs

T. brucei cultures at their exponential growth phase (10^5 cells mL^{-1}) were incubated with compounds or pentamidin (as reference compound) at their IC_{50} for 48 h; alternatively, the cells were exposed to their IC_{90} for different time periods. The shape and viability of the trypanosomes were monitored regularly by light microscopy after the addition of substances.

At the end of the incubation time, trypanosomes were fixed on ice for 10 min directly from the growth media with chilled 5 % glutaraldehyde and 8 % paraformaldehyde mixed 1:1 and 0.1 M sodium cacodylate. Fixed cells were then centrifuged at $400\times g$ for 20 min in Eppendorf tubes, and the supernatant was replaced with fresh fixative for further 30 min, without disturbing the pellet. This pellet was rinsed thrice in 0.1 M sodium cacodylate and fixed with 1 % aqueous osmium tetroxide. After rinsing, the cells were dehydrated in increasing concentrations of ethanol and incubated for 1 h in propylene oxide, followed by incubation for 1 h in a 1:1 mixture of propylene oxide and Epon-araldite and polymerizing at 60 °C for 48 h. Post-staining of sections was carried out with 1 % uranyl acetate for 30 min. Photographs were taken with a Zeiss EM10 transmission electron microscope at 100 kV, and scanned images were visualized using Adobe Photoshop (Field et al. 2004).

Ligand and descriptor calculation of the analyzed compounds

To expedite the discovery of chemical entities with effective anti-trypanosomal potency into the clinic, we analyzed 185 compounds of different structural classes, synthesized within the frame of our broad screening agenda, and tested for their activity against *T. brucei*.

The structure of all 185 ligands were converted from SMILES strings to 3D structures with the open-source software Open Babel (O'Boyle et al. 2011) (version 2.3.0). Schrödinger Maestro (Suite 2012: Maestro, version 9.3, Schrödinger, LLC, New York, NY, 2012) was used to visually inspect the 3D structures and create protomers at pH 7.0 +/− 2.0 with the tool Epik (Shelley et al. 2007), resulting in a total number of 230 structures. The protomers were energetically minimized with the MMFF94× force field to a maximum atom displacement below 0.001 Å, using MOE (Molecular Operating Environment, 2012.10; Chemical Computing Group Inc., 1010 Sherbooke St. West, Suite #910, Montreal, QC, Canada, H3A 2R7, 2012). The prevalent protomer at pH 7 was calculated using MoKa 1.1.0 (http://www.moldiscovery.com) (Milletti et al. 2007). The SMILES strings, as well as the anti-trypanosomal activities, macrophage cytotoxicites and selectivity indices (SI) of the 185 compounds are listed in Supplementary Material, Table 1.

Molecular descriptors were used to calculate LEi using the statistical framework R (R Core Team 2013) and ALOGPS from the Virtual Computational Chemistry Laboratory (Tetko et al. 2005). LEi represent the potency of compounds normalized by their physical properties, i.e., the number of non-hydrogen atoms (HA) (LE) or the lipophilicity (lipophilic ligand efficiency, LLE) with $LE=pIC_{50}$ / HA and $LLE=pIC_{50}$–ALogPS.

Table 1 summarizes the computed chemical properties of the compounds analyzed in the present study, according to "Lipinski's rule of 5". The table lists for each compound, the Polar Surface Area (PSA) and charge for titratable groups at neutral pH, as well as its difference referred to acidic cellular compartments of the cell. Moreover, the table summarizes the calculated chemical properties of commercial drugs (Supplementary Material, Fig. 1. Methyl triphenyl phosphonium, Mitotracker, Lysotracker, Chloroquine and Acridine Orange) known to target specific organelles (Tetko et al. 2005; Scott and Nicholls 1980; Okabe et al. 2012; Griffiths et al. 1988; Anderson and Orci 1988; De Duve et al. 1974; Mellman et al. 1986).

Results

The effect of compounds on *T. brucei* and macrophage growth

The activities against *T. brucei*, the cytotoxicities against macrophages (J774.1), and the selectivity indices (SI), defined as the ratio between the IC_{50} [J774.1] and IC_{50} [*T. brucei*], for all synthesized compounds are listed in the Supplementary Material, Table 1. Table 2 summarizes the values obtained for the compounds analyzed in the present study. The compounds exhibit IC_{50}s in the nanomolar range and are toxic against macrophages at higher concentrations; compounds **37**, **77**, and **88** have SI values higher than 200.

Table 1 Calculated chemical properties considered for analyzing the compounds according to the "Lipinski's rule of 5", Polar Surface Area and Charge

Target organelle									Mitochondria		Lysosome / acidic organelles		
Compound	2	4	15	37	68	69	77	88	MTPP	Mitotracker	Lysotracker	Chloroquine	Acridine orange
Heavy atom count	25	24	33	54	36	38	26	31	19	36	29	22	20
No of rings	2	1	4	6	3	4	2	3	3	8	4	2	3
H-bond donor	4	1	3	0	1	1	0	0	0	0	3	3	1
H-bond acceptor	4	3	3	4	8	7	0	0	0	2	1	1	2
MW, g/mol	340.42	333.38	443.54	864.75	497.45	523.92	369.25	410.32	277.23	496	399.25	319.87	265.35
PSA, Å^2 at pH 7.0	121.7	81.7	84.04	74.76	162.35	136.5	3.2203	3.2203	0	19.62	57.27	30.61	20.62
ALogPS	1.32	2.72	1.55	1.24	2.87	5.56	1.52	2.85	5.94	6.77	2.17	5.28	4.37
Charge at pH 7.0	2	0	0.92	2	0	0	1	1	1	1	0.97	1.7	0.94
Charge difference (pH 7 / 4.8)	0	0	0.15	0	0.12	0.11	0	0	0	0	0.03	0.27	0.11

The color code relates to the ranking of chemical properties between the different compounds (dark grey means high to light grey means low ranking). Ranking is a neutral term that organizes the order of the compounds related to the chemical properties, without any assessment

The effect of compounds on *T. brucei* morphology

To obtain insights on the mode of action of the selected compounds, we analyzed their effect on parasite morphology; the cells were stained with Giemsa after incubation with compounds for different periods. Then, 200 parasites were evaluated in two different experiments and by two individual researchers to enumerate parasites with slender or exploded morphology. Figure 2 summarizes the obtained results. Slender cells remained around 90 % in untreated wells, 10 % looked exploded. DMSO did not affect these percentages, although pentamidine (**2**) decreased the percentage of slender cells to 60 % and increased the percentage of exploded cells to 20 %. Compounds **37**, **68**, or **69** as well as **77** or **88** affected the parasites similarly to pentamidine. On the contrary, compounds **4** and **15** increased the percentage of exploded parasites to 50 % after 3 h of incubation and killed most parasites after 4 h. In control wells, 20 % of cells had duplicated kinetoplasts and nuclei, while in samples where parasites were incubated with compounds (**4**, **15**, or **37**); less than 20 % of the cells had these characteristics (data not shown).

Table 2 Anti-trypanosomal activities, cytotoxicities, and SI of selected compounds

Compound number	IC_{50} *T.brucei* (nM)	IC_{50} J774.1 (nM)	Selectivity index (SI)	IC_{90}[5] *T.brucei* (nM)
2	5.3	38,600	7283	12.8
4 [1]	510	18,000	35	1600
15 [1]	700	54,000	77	1600
37 [2]	500	>100,000	>200	1600
68 [3]	2710	>100,000	> 35	10,000
69 [3]	450	43,000	96	1600
77 [4]	350	>100,000	>285	1000
88 [4]	4.5	27,300	6,067	12

[1] Amino acid derivatives of fumaric acid and piperazine. [2] Bisquaternary bisnaphthalimides. [3] Piperidine derivatives, [4] *N*-Arylpyridinium salts. [5] Concentration used for selected electron microscopy experiments

The ultrastructure of treated cells

To refine the results on the phenotypic changes identified by light microscopy, we evaluated the effect of the compounds on the cell ultrastructure. *T. brucei* cultures at their exponential phase of growth (10^5 cells mL^{-1}) were incubated with compounds at their IC_{50} for 48 h. Most cells incubated with compounds had elevated amounts of vesicles resembling acidocalcisomes and irregularly shaped kinetoplasts and dilated mitochondria. Additionally, some compounds produced distortion of the endoplasmic reticula (**37**, **69** or **77**), atypical flagellar pocket (**15, 77** or **88**), membrane-whorl-like structures (**2**, **68** or **69**), appearance of vacuoles resembling lysosomes (**4**, **69** or **77**), and appearance of two flagella inside the flagellar pocket (**69**) (data not shown, see Supplementary Material, Fig. 2).

Parasites were also incubated with pentamidine (**2**) or the compounds at their IC_{90} for different periods (see Fig. 3). Incubation times were selected according to the shortest period needed to detect morphological changes in the parasites. Alterations in the endoplasmic reticula organization and appearance of membrane-whorl-like structures were apparent in cells treated with most compounds, presumably due to cell death. Additionally, most cells treated with **4**, **15**, **77,** or **88** were strongly degenerated, probably ongoing programmed cell death, with a lot of lipid droplets or translucent vacuoles.

Structural deterioration was manifest in mitochondria and kinetoplasts of pentamidine-treated cells as well as in those treated with **68** or **88**, respectively. The appearance of dark vesicles increased in cells treated with **4** or **15**. Interestingly, cells treated with pentamidine, **15**, **68**, or **77** revealed marked alterations in flagellar pocket morphology, and those treated

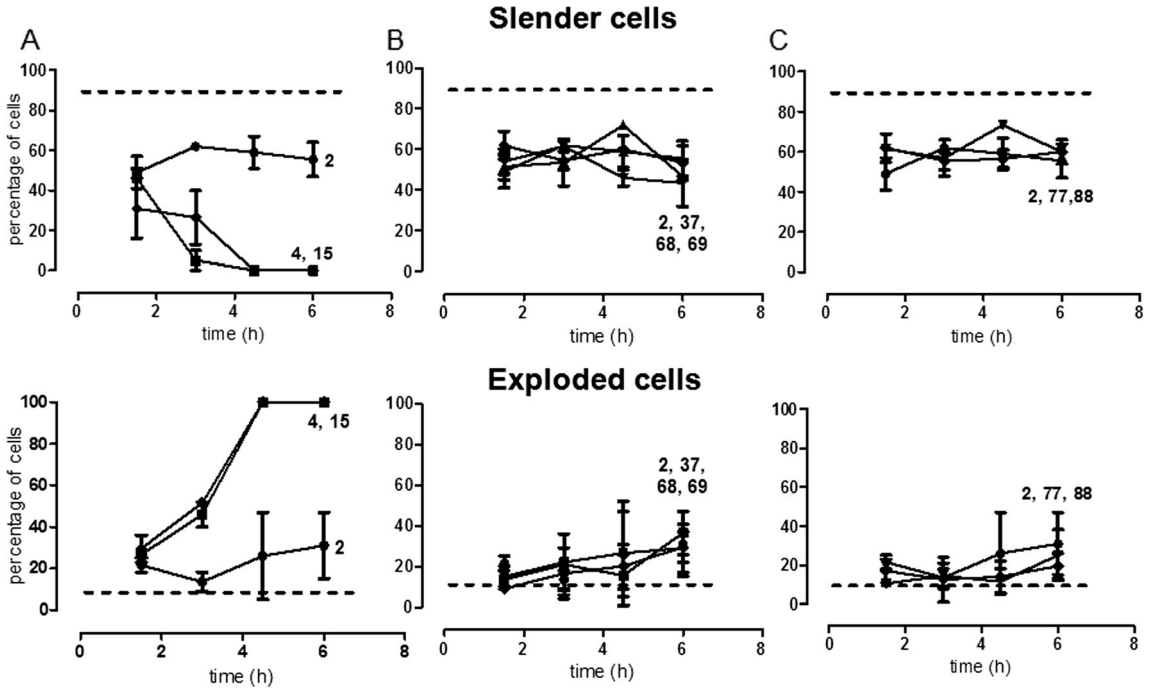

Fig. 2 Percentages of parasites with slender or exploded morphology. Effect of compounds. **a** Amino acid derivatives. **b** Bisquaternary bisnaphthalimides and piperidines. **c** *N*-Arylpyridinium salts. *Dashed line* represents the percentage of slender or exploded cells in untreated cells

with pentamidine or **15** had an irregular number of flagella inside the flagellar pocket. Cells treated with **4**, **77**, or **88** showed autophagocytic structures. Cells treated with **37** or **69** did not express significant morphological changes (data not shown).

Chemical properties and anti-protozoan activities

The previous results suggest that representative compounds of each class might have tropism for certain cellular targets. To gain additional knowledge in this direction, Table 1 summarizes their calculated physico-chemical properties according to "Lipinski's rule of 5", as well as the PSA and the charge of titratable groups at different pH values, referred to different trypanosomal cellular compartments. Compounds **37** (molecular weight of 865 Da) and **69** (molecular weight 524, predicted logP 5.56) violate—not dramatically—"Lipinski's rule of 5" in one or two parameters (Lipinski et al. 2001). The table also includes, for comparison, the corresponding properties of well-known commercial drugs that target specific organelles. The analysis suggests that (a) the pyridinium salts (**77** and **88**) share chemical properties with mitochondria-targeting molecules like triphenylphosphonium or mitotracker, being small cationic and hydrophobic molecules with almost no PSA and no titratable groups at the respective cellular or subcellular pH environment; (b) the amino acid derivative (**15**) resembles lysotracker, chloroquine or acridine orange, and acid organelle-targeting molecules; it becomes protonated in acidic compartments and has a medium-sized PSA. By contrast, the amino acid derivative with fumaric acid moiety (**4**) is uncharged at pH 4 to 8, but still has a medium-sized PSA; (c) the piperidone derivatives (**68** and **69**), which share properties with lysosome-targeting compounds, have the largest PSA of all compounds analyzed. Interestingly, this comparison suggests the existence of properties that might explain the results from electron microscopy experiments, indicating that the proposed cellular organelles might be targeted by the different compounds.

Ligand efficiency indices of the anti-trypanosomal compounds

The efficiency of drugs in vivo is driven by pharmacokinetics, bioavailability, and toxicity, characteristics which are mainly dependent on the compounds physico-chemical properties. Herein, we included ligand efficiency concepts referring to the impact of molecular weight and hydrophobicity on the potency of the molecules in the lead optimization process; we calculated ligand efficiency for all compounds. The results summarized in Fig. 4 illustrate for each family the relationship between the potency of the compounds normalized to the molecular weight (LE) and the potency of the compounds normalized to the lipophilicity (LLE) of the molecules. This easily understandable concept provides a mean to guide hit optimization not only by in vitro potency but also by drug likeness. Independent of the absolute values of LE and LLE,

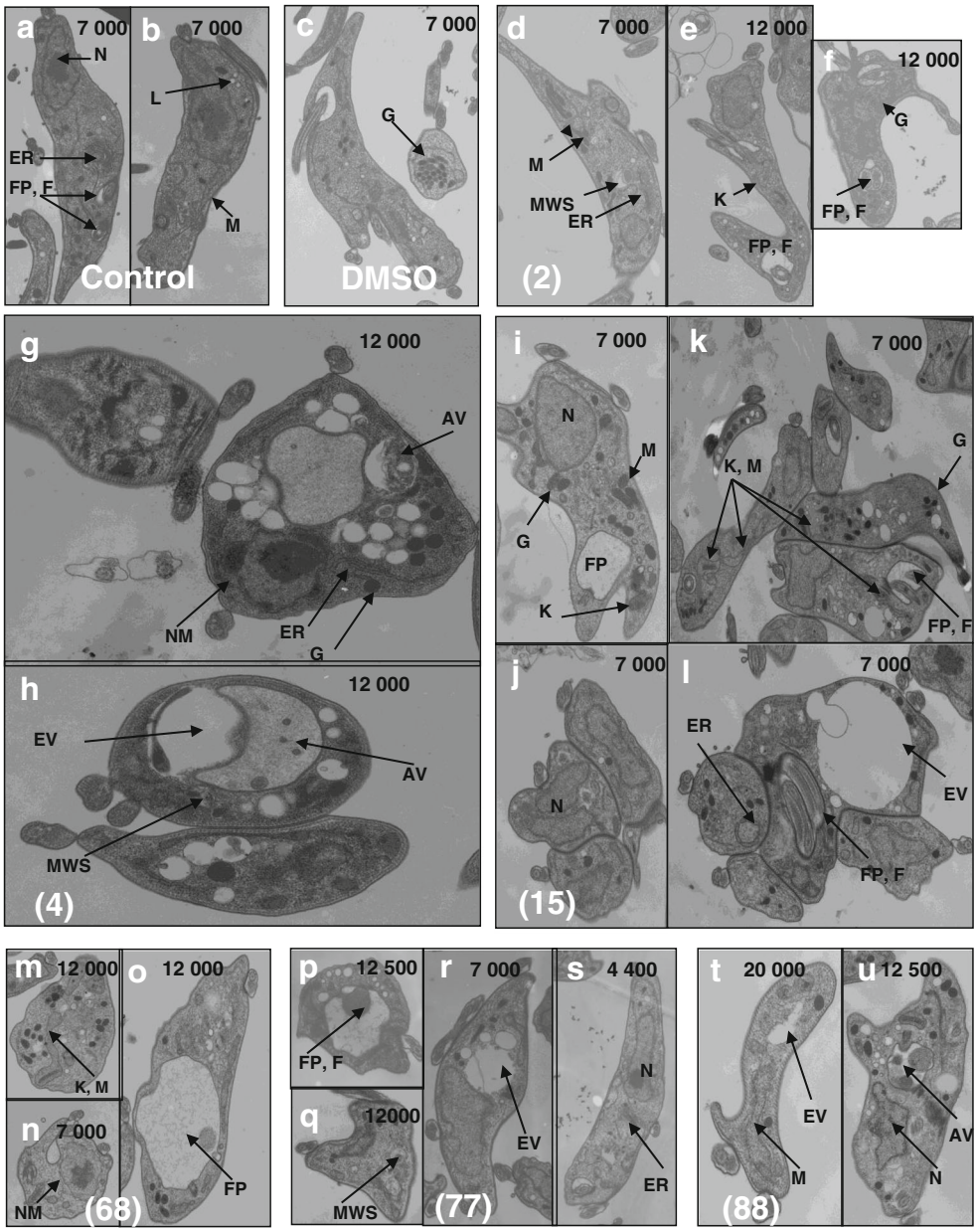

Fig. 3 Ultrastructural changes induced by compounds in *T. brucei* after different times of incubation at IC_{90}; (DMSO, **2**, **4**, **15**, **77**, and **88**, 7 h; **68**, 2.5 h). Images were captured with a Zeiss EM10 transmission electron microscope at 100 Kv at 7000–20,000-fold amplification, and scanned images were processed using Adobe Photoshop. The most obvious alterations in compound-treated cells were as follows: distorted flagellar pocket (f, k, o, p); dilated kinetoplasts and mitochondria (e, m, t); an elevated amount of dark vesicles (h, k, m, t); the appearance of membrane-whorl-like structures (d, h, q); altered endoplasmic reticulum (g, s); huge translucent and autophagic vacuoles (h, l, p, t, u); and altered nuclear membranes (g, n) as compared with control cells. Note the usual appearance of mitochondria, nuclei, and flagellar pockets in control and DMSO-treated cells (**a**, **b**, and **c**, respectively). Autophagic vesicles (*AV*); flagellum (*F*); flagellar pocket (*FP*); kinetoplast (*K*); lysosomes (*L*); mitochondria (*M*); membrane-whorl-like structures (*MWS*); nuclear membranes (*NM*); nuclei (*N*); dark vesicles (*V*)

the best compounds are always located in the upper right corner of the cloud.

Discussion

Failure of compounds during their developmental stage to get into clinical protocols is frequently produced by their unfavorable ADME properties and poor potential to permeate cell membranes. This situation has triggered the assessment of comprehensive properties of chemical entities in parallel to efficacy assays, to promote the identification of lead compounds or "all around" candidates, during their optimization stages. That is, in silico prediction of ADME properties by means of inexpensive specific software and ready-to-use tools, even before the synthesis of the compounds (Hou et al. 2007).

The potency of compounds of a given structural class, evaluated in enzyme- or cell-based assays, regularly positively correlates with increasing molecular weight and lipophilicity. However, often compound bioavailability decreases, and toxicity increases. Therefore, LEi, designed to correct potency of the compounds to their size and polarity, constitute a widely accepted drug development concept, helpful to guide drug likeness (Leeson and Springthorpe 2007). Hence, we analyzed the LE as a representation of activity normalized for the molecular weight and LLE as representation of activity

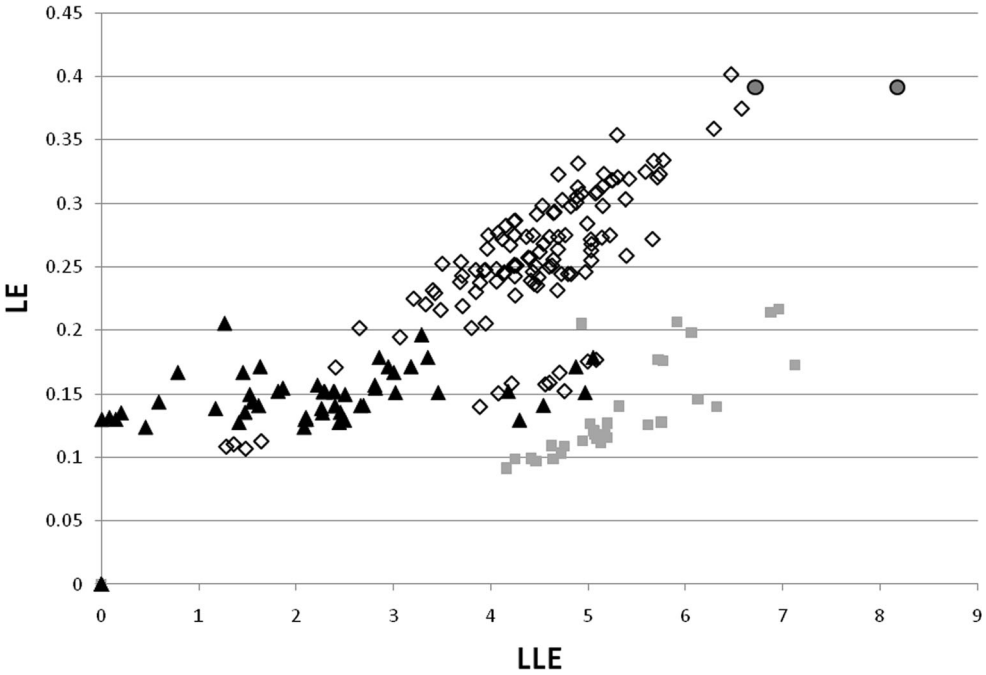

Fig. 4 Relationship between potency of the compounds normalized to molecular weight (LE) and potency of the compounds normalized to lipophilicity (LLE). Pyridinium salts are depicted as *diamonds*; bisnaphthalimides as *triangles*; piperidine derivatives as *squares*; eflornithine and pentamidine as *circles*

normalized for the lipophilicity for various families of compounds (bisquaternary bisnaphthalimides, piperidine derivatives, amino acids with fumaric acid and piperazine moieties, and *N*-Arylpyridinium salts as simplified derivatives of *N*,*C*-coupled naphthylisoquinolines (Tischer et al. 2010; Goebel et al. 2008; Ponte-Sucre et al. 2010) with potent antitrypanosomal activities and selectivities toward parasitic cells. The results demonstrate that within a structural family, it is possible to drive the formulation of compounds into the direction of highest activity and putatively acceptable ADME properties.

To gain insight into the mode of action, we performed studies with representative members of each compound class, with anti-trypanosomal activity at nanomolar concentrations, and good SI toward mammalian cells. We selected the best available compounds of their class at that given time. Table 2 lists the representative compounds IC_{50} against *T. brucei*, their cytotoxicities against J774.1 macrophages, and the corresponding SI values. The data demonstrates that **88** has an IC_{50} (4.5 nM) against *T. brucei* in the same range as pentamidine (**2**; 5.3 nM). The compounds can be organized according to their activity against *T. brucei* as follows: **88**<pentamidine (**2**)<<<**77**<**69**<**37**<**4**<**15**<**68** and according to their cytotoxicity against J774.1 macrophages as follows: **4**<**88**<pentamidine (**2**) <**69**<**15**<< **37**≈**68**≈**77**. As a consequence, the SI of these compounds increases as follows: **68**=**4**<**15**≈**69**< **37**≈**77**<<**88**≈pentamidine (**2**). In summary, the results suggest that *N*-Arylpyridinium salts **77** and **88** are the most active compounds against the parasites, exhibiting moderate to high SI, closely followed by the bisquaternary bisnaphthalimide **37**.

To advance on the phenomenological impact of these compounds, we analyzed their effect on the parasite morphology with light microscopy. Compounds **4** and **15** produced within 4-h dramatic morphological changes that ended up in the parasites losing their normal morphological appearance and looking exploded, suggesting that these derivatives induced dramatic changes very quickly. All other compounds tested herein, although seemingly more active than the fumaric acid or piperazine derivatives (lower IC_{50}, except **68**), appear to act in a slower manner.

Therefore, we analyzed which *T. brucei* organelles might be targeted by the drugs. This was done by means of electron microscopy. Most compounds produced elevated amounts of dark vesicles, and irregularly shaped kinetoplasts and dilated mitochondria, presumably as an unspecific secondary effect of cell damage in cells incubated for 48 h with compounds at their IC_{50} concentrations.

Cells treated with IC_{90} concentrations and shorter incubation times shared a common phenotype. That is, translucent vacuoles (of various sizes) in the cytoplasm, as well as lipid droplets, and membrane-whorl-like and autophagocytic structures, suggesting that the cells died, probably through apoptosis or necrosis.

Taking both experiments together, interesting outcomes could be described for the effect of some compounds. For example, *N*-Arylpyridinium salts may be targeting the flagellar pocket. In fact, previous experiments demonstrated that these compounds significantly increase cell volume and leads to a dramatic reduction of the flagellar pocket size (Ponte-Sucre et al. 2010). Additionally, they may be targeting mitochondria and kinetoplasts.

On the other hand, the bisquaternary bisnaphthalimides and piperidine derivatives may be targeting membranes of different intracellular organelles. This observation is in agreement with previous results suggesting that these compounds interfere with the biosynthesis of phosphatidylcholine, a phospholipid usually found in membranes (Tischer et al. 2010). Finally, the amino acid derivatives may preferentially target lysosomal compartments as has been previously described (Scory et al. 2000).

Compound structural properties determine in vivo their fate, absorbance, solubility, and distribution in the body fluids and ability to reach and enter the cell and eventually also specific organelles, to hit the target structure. Cellular compartments strongly differ in features like pH, membrane potential, and lipid composition. Thus, to analyze if organelle targeting and effect on parasite cells has any correlation with the structural properties of the selected compounds, we calculated their physico-chemical parameters, including the PSA and charge for titratable groups at different pH values referring to the different cellular compartments of the trypanosome. The comparison with chemical properties of commercial drugs known to target specific organelles supported at least partially the previous referred data. Additional experiments might be needed to clarify the herein found data.

Conclusions

We have furthered our knowledge on the activity of diverse compound classes and calculated ligand efficiencies for all compounds. ADME properties, membrane permeability, and interaction with metabolic pathways or organelles influence the pharmacokinetics, pharmacodynamics, and mechanism(s) of action of the compounds. Understanding these parameters seems essential for drug discovery in general and against one of the most neglected diseases on the planet, the African sleeping sickness. Our optimization process suggests that compounds to be developed might display better ADME properties for in vivo experiments.

From the morphological and ultrastructural effects exerted by compounds, our results suggest that different compounds target distinct organelles. Additionally, the comparison with commercial drugs allows us to suggest that their structural parameters may facilitate targeting in correlation with specific organelle features—such as membrane composition and charge (e.g., mitochondria have a negatively charged membrane), membrane potential, and internal pH (like acidic lysosomes). This analysis might prove to be fundamental for refining the screening of potential candidates that should go into animal and preclinical studies and further development.

Acknowledgments This work was supported by a grant of the Deutsche Forschungsgemeinschaft (DFG Collaborative Research Center 630, "Recognition, Preparation, and Functional Analysis of Agents against Infectious Diseases"; projects A1, A2, A4, B8, C7, Z1, and QM). We thank Daniela Bunsen and Claudia Gehrig from the University of Würzburg, (Core Unit for Electron Microscopy) and Martina Schultheis, Elena Katzowitsch, and Svetlana Sologub (Institute for Molecular Infection Biology, University of Würzburg) for the technical assistance. APS had the support of the Alexander von Humboldt Foundation, Germany.

References

Anderson RG, Orci L (1988) A view of acidic intracellular compartments. J Cell Biol 106:539–543

Balaban AT, Boulton AJ (1969) 2,4,6-Trimethylpyrylium tetrafluoroborate. Org Synth 49:121–122

Bender W, Staudt M, Trankle C, Mohr K, Holzgrabe U (2000) Probing the size of a hydrophobic binding pocket within the allosteric site of muscarinic acetylcholine M2-receptors. Life Sci 66:1675–1682

Braña MF, Ramos A (2001) Naphthalimides as anti-cancer agents: synthesis and biological activity. Curr Med Chem Anticancer Agents 1: 237–255

Breuning A, Degel B, Schulz F, Büchold C, Stempka M, Machon U et al (2010) Michael acceptor based antiplasmodial and antitrypanosomal cysteine protease inhibitors with unusual amino acids. J Med Chem 53:1951–1963

Bringmann G, Hoerr V, Holzgrabe U, Stich A (2003) Antitrypanosomal naphthylisoquinoline alkaloids and related compounds. Pharmazie 58:343–346

Brun R, Blum J, Chappuis F, Burri C (2010) Human African trypanosomiasis. Lancet 375:148–159

Buechold C, Hemberger Y, Heindl C, Welker A, Degel B, Pfeuffer T, Staib P, Schneider S, Rosenthal PJ, Gut J, Morschhaeuser J, Bringmann G, Schirmeister T et al (2011) New *cis*-configured aziridine-2-carboxylates as aspartic acid protease inhibitors. Chem Med Chem 6:141–152

De Duve C, De Barsy T, Poole B, Trouet A, Tulkens P, Van Hoof F (1974) Lysosomotropic agents. Biochem Pharmacol 24:2495–2531

Efremov RG, Chugunov AO, Pyrkov TV, Priestle JP, Arseniev AS, Jacoby E (2007) Molecular lipophilicity in protein modeling and drug design. Curr Med Chem 14:393–415

Field MC, Allen CL, Dhir V, Goulding D, Hall BS, Morgan GW et al (2004) New approaches to the microscopic imaging of *Trypanosoma brucei*. Microsc Microanal 10:621–636

Goebel T, Ulmer D, Projahn H, Klöckner J, Heller E, Glaser M et al (2008) In search of novel agents for therapy of tropical diseases and human immunodeficiency virus. J Med Chem 51:238–250

Griffiths G, Hoflack B, Simons K, Mellman I, Kornfeld S (1988) The mannose 6-phosphate receptor and the biogenesis of lysosomes. Cell 52:329–341

Hou T, Wang J, Zhang W, Xu X (2007) ADME evaluation in drug discovery. 6. Can oral bioavailability in humans be effectively predicted by simple molecular property-based rules? J Chem Inf Model 47:460–463

Leeson P, Springthorpe B (2007) The influence of drug-like concepts on decision-making in medicinal chemistry. Nat Rev Drug Discov 6: 881–890

Lipinski CA, Lombardo F, Dominy BW, Feeney PJ (2001) Experimental and computational approaches to estimate solubility and permeability in drug discovery and development settings. Adv Drug Deliv Rev 46:3–26

Mellman I, Fuchs R, Helenins A (1986) Acidification of the endocytic and exocytic pathways. Annu Rev Biochem 55:663–700

Milletti F, Storchi L, Sforna G, Cruciani G (2007) New and original pKa prediction method using grid molecular interaction fields. J Chem Inform Model 47:2172–2181

Muth M, Hoerr V, Glaser M, Ponte-Sucre A, Moll H, Stich A, Holzgrabe U (2007) Antitrypanosomal activity of quaternary naphthalimide derivatives. Bioorg Med Chem Lett 17:1590–1593

O'Boyle NM, Banck M, James CA, Morley C, Vandermeersch T, Hutchison GR (2011) Open Babel: an open chemical toolbox. J Chem Inform 3:1–14

Okabe K, Inada N, Gota C, Harada Y, Funatsu T, Uchiyama S (2012) Intracellular temperature mapping with a fluorescent polymeric thermometer and fluorescence lifetime imaging microscopy. Nat Commun 3:705

Ponte-Sucre A, Faber JH, Gulder T, Kajahn I, Pedersen SE, Schultheis M, Bringmann G, Moll H (2007) Activities of naphthylisoquinoline alkaloids and synthetic analogs against *Leishmania major*. Antimicrob Agents Chemother 51:188–194

Ponte-Sucre A, Gulder T, Wegehaupt A, Albert C, Rikanović C, Schaeflein L et al (2009) Structure-activity relationship and studies on the molecular mechanism of leishmanicidal N, C-coupled arylisoquinolinium salts. J Med Chem 52:626–636

Ponte-Sucre A, Gulder TA, Vollmers G, Bringmann G, Moll H (2010) Alterations to the structure of *Leishmania major* induced by *N*-arylisoquinolines correlate with compound accumulation and disposition. J Med Microbiol 59:69–75

Ponte-Sucre A, Díaz E, Padrón-Nieves M (2012) Quantitative structure-activity analysis of leishmanicidal compounds. In Ramalho TC, Freitas MP, and da Cunha EFF, editors. Chemoinformatics: Directions toward combating neglected diseases. Bentham Science Publishers; p. 33–49

Rippert AJ, Hansen HJ (1995) Synthesis of 4,6,8-trisubstituted methyl azulene-2-carboxylates. Helv Chim Acta 78:238–241

R Core Team (2013) R: a language and environment for statistical computing. R Foundation for Statistical Computing, Vienna, Austria. ISBN 3-900051-07-0, URL http://www.R-project.org/.

Sami SM, Dorr RT, Alberts DS, Sólyom AM, Remers WA (2000) Analogues of amonafide and azonafide with novel ring systems. J Med Chem 43:3067–3073

Scory S, Stierhof YD, Caffrey CR, Steverding D (2000) The cysteine proteinase inhibitor Z-Phe-Ala-CHN2 alters cell morphology and cell division activity of *Trypanosoma brucei* bloodstream forms in vivo. Kinetoplastid Biol Dis 6:2

Scott ID, Nicholls DG (1980) Energy transduction in intact synaptosomes. Influence of plasma-membrane depolarization on the respiration and membrane potential of internal mitochondria determined in situ. Biochem J 186:21–33

Shelley JC, Cholleti A, Frye LL, Greenwood JR, Timlin MR, Uchimaya M (2007) Epik: a software program for pK a prediction and protonation state generation for drug-like molecules. J Comput Aided Mol Des 21:681–691

Smith TK, Bûtikofer P (2010) Lipid metabolism in *Trypanosoma brucei*. Mol Biochem Parasitol 172:66–79

Steverding D, Tyler KM (2005) Novel antitrypanosomal agents. Expert Opin Investig Drugs 14:939–955

Stich A, Ponte-Sucre A, Holzgrabe U (2013) Do we need new drugs against human *African trypanosomiasis*? Lancet Infect Dis 13:733–734

Tetko IV, Gasteiger J, Todeschini R, Mauri A, Livingstone D, Ertl P et al (2005) Virtual computational chemistry laboratory—design and description. J Comput Aided Mol Des 19:453–463

Tischer M, Sologub L, Pradel G, Holzgrabe U (2010) The bisnaphthalimides as new active lead compounds against *Plasmodium falciparum*. Bioorg Med Chem 18:2998–3003

Verkman AS (2004) Drug discovery in academia. Am J Physiol Cell Physiol 286:C465–C474